Verification of the INL/COMBINE7 Neutron Energy Spectrum Code

International Conference on Reactor Physics, Nuclear Power: A Sustainable Resource

Barry D. Ganapol
Woo Y. Yoon
David W. Nigg

September 2008

The INL is a
U.S. Department of Energy
National Laboratory
operated by
Battelle Energy Alliance

INL
Idaho National
Laboratory

Verification of the INL/**COMBINE**7 neutron energy spectrum code

Barry D. Ganapol[a,*], Woo Y. Yoon[b], David W. Nigg[b]

[a]University of Arizona, Tucson, AZ
[b]Idaho National Laboratory, Idaho Falls, ID

Abstract

We construct semi-analytic benchmarks for the neutron slowing down equations in the thermal, resonance and fast energy regimes through mathematical embedding. The method features a fictitious time-dependent slowing down equations solved via Taylor series expansion over discrete "time" intervals. Two classes of benchmarks are considered– the first treats methods of solution and the second the multigroup approximation itself. We present several meaningful benchmark methods comparisons with the **COMBINE7** energy spectrum code and a simple demonstration of convergence of the multigroup approximation.

1. Introduction

Cross section generation is the basis of reliable multigroup reactor physics calculations. The multigroup method allows efficient use of the enormous amount of nuclear physics cross section information to design and predict the behavior of present-day and future nuclear reactors. The multigroup cross section generation process involves several stages, each requiring quality control measures to ensure reliability, i.e., accuracy and proper performance. In particular, the microscopic cross section energy variation for participating nuclei must be available either theoretically or experimentally. This requires experimental validation and theoretical interpolation/extrapolation based on our current knowledge. In addition, verification of proper recording and archiving of the nuclear data generated is essential. The second step in the generation of useable cross section data is its reduction to a suitable computational form, i.e., processing **ENDF/B** point cross sections to generate multigroup cross sections for application. In general, the enormity of the pointwise experimental nuclear data available in its basic evaluated form generally precludes its use directly in reactor physics computations—hence the need for an intervening multigroup format. The multigroup approximation, requires discretization of the energy variable into discrete groups, and, as such, creates discretization error. We can generate a multigroup formation by integrating the nuclear data assuming a weighting flux independent of information of a particular reactor configuration. This leads to a set of multigroup cross sections usually between 100 and 300 groups as well as the corresponding flux spectrum for the specified material mix. The last phase of cross section generation includes reactor specific information, to generate representative few-

Corresponding author, ganapol@cowboy.ame.arizona.edu
Tel: 520/621-4728; Fax: 520/621-8191.

group homogenized cross section sets for speedy, but representative reactor physics computations.

Therefore, multigroup cross section generation requires energy discretization and the assumption of a "weighting flux spectrum". However, the fission spectrum in the fast energy range, the $1/E$ slowing down spectrum and detailed balance at thermal energies are relatively "good guesses" which give representative results.

We can identify several benchmark types for verification and assessment of a cross section generation package. The most common benchmark applies to the numerical method used to solve the slowing down equations. This benchmark addresses the question: Given the multigroup approximation, how accurately are we solving the slowing down equations? We can conceive of a second benchmark however, to address the question: How well does the multigroup approximation represent the solution to the slowing down equations? In the following, we address the first question with regard to the **INL/COMBINE7** [Grimesey, 1990] spectrum code for cross section generation, and then we investigate the convergence of the multigroup approximation.

2. Benchmarking the COMBINE7 cross section generation code

2.1. *The **COMBINE**7 solution to the slowing down equations*

The multigroup B_N equations in **COMBINE7** for the nth Legendre flux moment (per lethargy) are

$$\phi_n^g =$$

$$= \sum_{l=0}^{L} (2l+1) \left[\frac{A_{nl}^g}{\Sigma_g} \right] \sum_{g'=1}^{G} \Sigma_{sl}^{g'\to g} \phi_l^{g'} \frac{\Delta g'}{\Delta g} + \qquad (1)$$

$$+ \frac{A_{n0}^g}{\Sigma_g} \frac{\chi^g}{\Delta g}$$

where

$$\phi_n^g = \int_{E_g}^{E_{g-1}} \phi_n(E) \frac{dE}{E} / \Delta_g$$

$$\Delta g = \int_{E_g}^{E_{g-1}} \frac{dE}{E}$$

and

$$A_{nl}^g \equiv \frac{(i)^{l-n}}{2} \int_{-1}^{1} \frac{P_n(\mu) P_l(\mu)}{1 - \frac{iB\mu}{\Sigma_g}} d\mu .$$

$\Sigma_{sl}^{g'\to g}$ is the group transfer scattering cross section from group g' to-group g. In addition, we assume an isotropic source. The B_3 solution is given by the following matrix equation for each energy group g:

$$\left[\mathrm{I} - \boldsymbol{C}_g \right] \boldsymbol{\Phi}_g = \boldsymbol{R}_g \qquad (2)$$

$$\boldsymbol{\Phi}_g = \left[\phi_0^g, \phi_1^g, \phi_2^g, \phi_3^g \right]^T$$

$$C_{nl}^g = (2l+1) \frac{A_{nl}^g}{\Sigma_g} \Sigma_{sl}^{g\to g}$$

$$\boldsymbol{R}_g = \left[R_0^g, R_1^g, R_2^g, R_3^g \right]^T$$

where

$$R_n^g = \frac{A_{n0}^g}{\Sigma_g} \frac{\chi^g}{\Delta g} +$$

$$+ \sum_{l=0}^{3} (2l+1) \frac{A_{nl}^g}{\Sigma_g} \sum_{\substack{g'=1 \\ g' \neq g}}^{G} \Sigma_{sl}^{g'\to g} \phi_l^{g'} \frac{\Delta g'}{\Delta g}$$

When there is no thermal upscattering, we solve for the flux moments by Gauss elimination, sweeping from the highest energy to the lowest. When the thermal upscattering is present, we obtain the moments by combination of Gauss elimination and Gauss-Seidel iteration.

2.2. *An alternative solution to the slowing down equations*

In general, the infinite medium, multigroup transport equation,

2

$$\sum_{l=0}^{L} \left[\Sigma_g \delta_{ml} - (2l+1) A_{mlg} \Sigma_{sl}^{g' \to g} \right] F_{lg} =$$

$$= \sum_{l=0}^{L} (2l+1) A_{mlg} \sum_{g'=1}^{G} \Sigma_{sl}^{g' \to g} F_{lg'} \qquad (3)$$

$$+ S_{0g} A_{m0g}, \quad m = 0,1,2,...,L,$$

for the Legendre moments of the multigroup flux, now defined as $F_{lg} \equiv \phi_l^g \Delta g$, are appropriate in both the fast and thermal energy regions. In Eq.(3), as in Eq.(1),

$$A_{mlg} \equiv i^{l-m} T_{ml} \left(-\alpha_{B_L g} \right)$$

with

$$\alpha_{B_L g}(u) \equiv \frac{B_L}{\Sigma_g}$$

$$T_{ml}(-z) \equiv \frac{1}{2} \int_{-1}^{1} d\mu \frac{P_m(\mu) P_l(\mu)}{1 - iz\mu}.$$

B is the assumed buckling $\sqrt{B^2}$. Note that fission is included through a more inclusive definition of the transfer cross section for $l = 0$.

Here, we focus only on the moments $l = 0,1$, the flux and current respectively, the equations for which are

$$\Sigma_g F_{0g} + B_L F_{1g} = \sum_{g'=1}^{G} \Sigma_{s0gg'} F_{0g'} + S_{0g} \qquad (4a)$$

$$-\frac{B_L}{3} F_{0g} + \gamma_g \Sigma_g F_{1g} = \sum_{g'=1}^{G} \Sigma_{s1gg'} F_{1g'}, \qquad (4b)$$

where

$$\gamma_g \equiv \frac{T_g \alpha_{Lg}^2}{3(1 - T_g)}, \quad T_g \equiv \frac{Tan^{-1}(\alpha_{Lg})}{\alpha_{Lg}}.$$

Equations (4) give the flux moments as a group vector found by matrix inversion for G on the order of 300. While direct inversion is certainly possible as performed in **COMBINE7**, we seek an alternative method to provide an independent solution.

2.2.1 Embedded equations

We begin by arbitrarily adding time derivatives to Eqs.(4) to give

$$\varepsilon_0 \frac{\partial F_{0g}(t)}{\partial t} + \Sigma_g F_{0g}(t) + B F_{1g}(t) = \qquad (5a)$$

$$= \sum_{g'=1}^{G} \Sigma_{s0}^{g' \to g} F_{0g'}(t) + S_{0g}$$

$$\varepsilon_1 \frac{\partial F_{1g}(t)}{\partial t} - \frac{B}{3} F_{0g}(t) + \qquad (5b)$$

$$+ \gamma_g \Sigma_g F_{1g}(t) = \sum_{g'=1}^{G} \Sigma_{s1}^{g' \to g} F_{1g'}(t).$$

This is a purely numerical artifice to iterate to the solution through a fictitious time t. ε_0 and ε_1 are parameters to accelerate convergence of the iterative process, if possible. It is evident, therefore, that the desired solution is the "stationary distribution" associated with Eqs.(5) for a source constant in time.

2.2.2. Taylor series solution

We obtain the solution to Eqs.(5) through a method called continuous analytical continuation (CAC) [Fairen, 1988], by expressing $F_{lg}(t)$, as a Taylor series about the beginning of the rth subinterval, $t_{r-1} \leq t \leq t_r$. The series coefficients are determined recursively. Thus, the desired solution is the "time-asymptotic" value of F_{lg} as t approaches infinity. We have implemented the CAC solution in the **THERM** code whose results we now compare to **COMBINE7** results.

2.3. Benchmarking **COMBINE7**

The first of several **COMBINE7** verification exercises is for slowing down to thermal energies in a graphite/Pu-239 mixture. Using **COMBINE7**, we constructed a 100-group multigroup cross section set from **ENDF/B** for neutrons slowing down from the fast region to the epithermal/thermal region. The energy range is from $3.4824 ev$ to $10^{-5} ev$. The neutrons enter the energy range from a fission

source located at high-energy. We ran the identical case with the independent **THERM** code. The **COMBINE7** output provided the total cross sections, elastic down scatter and thermal upscatter matrices. This limited the accuracy of the nuclear data to 4 places (5 digits) since we took data directly from the **COMBINE7** output. No additional data other than the energy grid and buckling (B^2), here 10^{-4}, was required. We normalized the flux to its integral over the specified energy interval.

Figure 1a shows the direct comparison of the group fluxes for the two calculations for a factor of 1000 difference in density between the fuel and moderator. To the graphical norm, they are identical. In addition, the influence of the Pu-239 resonance is evident at $0.2956 ev$. Figure 1b emphasizes the agreement through the relative error indicating nearly 5-digit agreement.

Since we also have results for graphite without resonance, we can perform the following analysis to illustrate graphically the impact of the resonance with increasing fissile concentration. By assuming a fixed graphite density, any macroscopic group cross section containing Pu-239 of density N_r is

$$\Sigma_g\left(N_r\right) = \Sigma_{Gg} + \frac{N_r}{N_{r0}}\left[\Sigma_g\left(N_{r0}\right) - \Sigma_{Gg}\right]. \quad (6)$$

Σ_{Gg} is the graphite group cross section without resonance and N_{r0} is the Pu-239 density of the above resonance calculation. Figure 2 illustrates the variation of the flux with Pu-239 density as given by the **THERM** code. The gradual appearance of the absorbing effect of the resonance is evident.

3. Analytical cross section generation

We can conceive of a second benchmark investigation concerning the convergence of the multigroup approximation itself. If we assume elastic scattering or a single level Breit- Wigner resonance, we can numerically investigate convergence. In the following, we will develop an analytical set of group parameters for elastic scattering.

3.1 Elastic scattering

3.1.1. Total cross sections

We begin with the following definition of the group scattering and absorption cross sections:

$$\sigma_{ig} \equiv \int_{E_g}^{E_{g-1}} dE g\left(E\right)\sigma_i\left(E\right) \quad (7a)$$

$i = a(bsorption), s(cattering),$

where we assume a $1/E$ weighting flux,

$$g\left(E\right) \equiv \frac{\alpha_{0g}}{E}, \quad E_g \leq E \leq E_{g-1}. \quad (7b)$$

Since

$$\int_{E_g}^{E_{g-1}} dE g\left(E\right) \equiv 1, \quad (7c)$$

we have

$$\alpha_{0g} = \left[\ln\left(\frac{E_{g-1}}{E_g}\right)\right]^{-1} = \frac{1}{\Delta u_g}, \quad (7d)$$

which we use in the determination of the transfer cross sections. Thus, Eq.(7a) gives the total macroscopic cross section for a nuclide of atom density N in group g

$$\Sigma_g \equiv N\left[\sigma_{ag} + \sigma_{sg}\right], \quad (8a)$$

and similarly for the macroscopic scattering and absorption cross sections

$$\Sigma_{sg} = N\sigma_{sg}, \quad \Sigma_{ag} = N\sigma_{ag}. \quad (8b)$$

σ_{ig} is the average value in the group interval.

3.1.2. Transfer cross section

The determination of the transfer cross section is much more challenging but still a relatively simple analytical exercise. The g'- group to g group transfer cross section is

$$\Sigma_{sgg'} \equiv$$
$$\equiv \int_{E_g}^{E_{g-1}} dE \int_{E_{g'}}^{E_{g'-1}} dE' \Sigma_s\left(E' \rightarrow E\right) g_{g'}\left(E'\right), \quad (9)$$

where for elastic scattering

$$\Sigma_s\left(E' \to E\right) =$$
$$= \frac{1}{(1-\alpha)E'} \Sigma_s \rho\left(E', E\right) \qquad (10a)$$

and

$$\rho\left(E', E\right) \equiv$$
$$\equiv \begin{cases} 1, & \alpha E' \leq E \leq E \\ 0, & \text{otherwise} \end{cases} = \qquad (10b)$$
$$= \theta\left(E - \alpha E'\right) - \theta\left(E - E'\right)$$

with

$$\alpha \equiv \left[\frac{A-1}{A+1}\right]^2. \qquad (10c)$$

A is the atomic mass number of the scattering/absorbing nuclide and the Heaviside step function is

$$\theta\left(u\right) \equiv \begin{cases} 1, & u > 0 \\ 0, & u < 0. \end{cases}$$

Therefore, the group-to-group transfer cross section becomes

$$\Sigma_{sgg'} \equiv$$
$$\equiv \frac{\alpha_{0g'}\Sigma_{sg'}}{1-\alpha} \int_{E_{g'}}^{E_{g'-1}} \frac{dE'}{E'^2} \int_{E_g}^{E_{g-1}} dE\,\rho\left(E', E\right) \qquad (11)$$

This integral is rather difficult to evaluate numerically because of the discontinuities in the integrand. However, from the following integral relation for $\gamma_2 \geq \gamma_1$, we now show that

$$\int_{\gamma_1}^{\gamma_2} dEf\left(E\right)\theta\left(E - \beta\right) =$$
$$= \theta\left(\gamma_2 - \beta\right) \int_{\beta}^{\gamma_2} dEf\left(E\right) - \qquad (12)$$
$$- \theta\left(\gamma_1 - \beta\right) \int_{\beta}^{\gamma_1} dEf\left(E\right)$$

We see this by decomposing the original integral into

$$\int_{\gamma_1}^{\gamma_2} dEf\left(E\right)\theta\left(E - \beta\right) = I^+ - I^-,$$

where

$$I^+ \equiv \int_0^{\gamma_2} dEf\left(E\right)\theta\left(E - \beta\right)$$
$$I^- \equiv \int_0^{\gamma_1} dEf\left(E\right)\theta\left(E - \beta\right).$$

Then, through integration by parts, the first integral becomes

$$I^+ \equiv \int_0^E dE'f\left(E'\right)\theta\left(E - \beta\right)\Big|_0^{\gamma_2} -$$
$$- \int_0^{\gamma_2} dE \int_0^E dE'f\left(E'\right)\delta\left(E - \beta\right)$$

with the delta function

$$\delta\left(E - \beta\right) \equiv \frac{d\theta\left(E - \beta\right)}{dE}.$$

Therefore,

$$I^+ \equiv \theta\left(\gamma_2 - \beta\right) \int_0^{\gamma_2} dE'f\left(E'\right) -$$
$$- \theta\left(\gamma_2 - \beta\right) \int_0^{\beta} dE'f\left(E'\right)$$

and simplifying

$$I^+ \equiv \theta\left(\gamma_2 - \beta\right) \int_{\beta}^{\gamma_2} dE'f\left(E'\right)$$

Thus, through identification of γ_1 with γ_2 the second integral is

$$I^- \equiv \theta\left(\gamma_1 - \beta\right) \int_{\beta}^{\gamma_1} dE'f\left(E'\right)$$

With these integrals, we have

$$\int_{E_g}^{E_{g-1}} dE\, \rho\left(E', E\right) =$$

$$
\begin{aligned}
&= \left(E_{g-1} - \alpha E'\right)\theta\left(E_{g-1} - \alpha E'\right) - \\
&- \left(E_g - \alpha E'\right)\theta\left(E_g - \alpha E'\right) - \\
&- \left(E_{g-1} - E'\right)\theta\left(E_{g-1} - E'\right) + \\
&+ \left(E_g - E'\right)\theta\left(E_g - E'\right);
\end{aligned}
\tag{13}
$$

giving

$$
\Sigma_{sgg'} \equiv \frac{\alpha_{0g'}\Sigma_{sg'}}{1-\alpha} \int_{E_{g'}}^{E_{g'-1}} \frac{dE'}{E'^2} \Box
$$

$$
\Box
\begin{cases}
-\left(E_{g-1} - E'\right)\theta\left(E_{g-1} - E'\right) + \\
+\left(E_g - E'\right)\theta\left(E_g - E'\right) + \\
+\left(E_{g-1} - \alpha E'\right)\theta\left(E_{g-1} - \alpha E'\right) - \\
-\left(E_g - \alpha E'\right)\theta\left(E_g - \alpha E'\right)
\end{cases}
\tag{14}
$$

Again, the integrand contains discontinuities and presents numerical difficulty. We can still perform the integration analytically however, since for $\gamma_2 \geq \gamma_1$

$$
\int_{\gamma_1}^{\gamma_2} dE'\, f\left(E'\right)\theta\left(\beta - \gamma E'\right) =
$$

$$
\begin{aligned}
&= \theta\left(\beta - \gamma\gamma_2\right) \int_{\beta/\gamma}^{\gamma_2} dE'\, f\left(E'\right) + \\
&+ \theta\left(\beta - \gamma\gamma_1\right) \int_{\gamma_1}^{\beta/\gamma} dE'\, f\left(E'\right),
\end{aligned}
\tag{15}
$$

where (now) $\gamma_1 \equiv E_{g'}$, $\gamma_2 \equiv E_{g'-1}$; and Eq.(14) is composed of four such integrals exactly of this form with different limits. We obtain an analytical expression from Eq.(12) by noting

$$
\int_{\gamma_1}^{\gamma_2} dE'\, f\left(E'\right)\theta\left(\beta - \gamma E'\right) =
$$

$$
= \int_{\gamma_1}^{\gamma_2} dE'\, f\left(E'\right)\theta\left(\beta/\gamma - E'\right)
$$

$$
= \int_{\gamma_1}^{\gamma_2} dE'\, f\left(E'\right)\left[1 - \theta\left(E' - \beta/\gamma\right)\right]
$$

The first term is expressed directly by Eq.(12) and the second member of the second integral is

$$
\int_{\gamma_1}^{\gamma_2} dE'\, f\left(E'\right)\theta\left(E' - \beta/\gamma\right) =
$$

$$
\begin{aligned}
&= \theta\left(\gamma\gamma_2 - \beta\right) \int_{\beta/\gamma}^{\gamma_2} dE'\, f\left(E'\right) + \\
&+ \theta\left(\gamma\gamma_1 - \beta\right) \int_{\gamma_1}^{\beta/\gamma} dE'\, f\left(E'\right),
\end{aligned}
$$

but the first member is

$$
\int_{\gamma_1}^{\gamma_2} dE'\, f\left(E'\right) =
$$

$$
= \int_{\gamma_1}^{\beta/\gamma} dE'\, f\left(E'\right) + \int_{\beta/\gamma}^{\gamma_2} dE'\, f\left(E'\right).
$$

The final expression, Eq.(15), is obtained by noting

$$
\theta\left(\gamma\gamma_2 - \beta\right) = 1 - \theta\left(\beta - \gamma\gamma_2\right)
$$

$$
\theta\left(\gamma\gamma_1 - \beta\right) = 1 - \theta\left(\beta - \gamma\gamma_1\right).
$$

Table 1 gives appropriate β and γ for the integrals in Eq(14) (in order of appearance) with

$$
f\left(E'\right) \equiv \frac{1}{E'^2}\left(\beta - \gamma E'\right).
$$

Table 1
Parameters for Integral Evaluation in Eq.(14)

Term	β	γ
1	E_{g-1}	1
2	E_g	1
3	E_{g-1}	α
4	E_g	α

Thus, we must only evaluate the following integral:

6

$$T\left(\nu_1, \nu_2\right) \equiv \int_{\nu_1}^{\nu_2} \frac{dE'}{E'^2}\left(\beta - \gamma E'\right), \qquad (16)$$

where

$$\nu_1 = \beta/\gamma \text{ or } E_{g'}$$
$$\nu_2 = E_{g'-1} \text{ or } \beta/\gamma,$$

giving

$$T\left(\nu_1, \nu_2\right) \equiv$$
$$\equiv \beta\left[\frac{1}{\nu_1} - \frac{1}{\nu_2}\right] - \gamma \ln\left(\frac{\nu_2}{\nu_1}\right). \qquad (17)$$

Each of the four integrals therefore is of the form

$$\int_{E_{g'}}^{E_{g'-1}} \frac{dE'}{E'^2}\left(\beta - \gamma E'\right)\theta\left(\beta - \gamma E'\right) =$$
$$= \theta\left(\beta - \gamma E_{g'-1}\right)T\left(\beta/\gamma, E_{g'-1}\right) + \qquad (18)$$
$$+ \theta\left(\beta - \gamma E_{g'}\right)T\left(E_{g'}, \beta/\gamma\right)$$

completing the analytic determination of the group-to-group transfer cross section.

3.1.3. Slowing down source

To complete the analysis, we introduce the concept of a slowing down source form outside an energy interval. By considering only isotropic scattering, the slowing down equations for the flux $\phi(E)$ is

$$\Sigma(E)\phi(E) =$$
$$= \int_0^{E_0} dE'\Sigma_s\left(E' \to E\right)\phi\left(E'\right) + S(E) \qquad (19)$$

Say, we want to interrogate the following slowing down interval $\left[E_i, E_f\right]$:
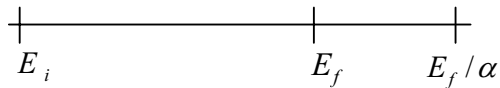
Then, neutrons can slow down into this interval from $\left[E_f, E_f/\alpha\right]$. If Eq.(19) is written as

$$\Sigma(E)\phi(E) = \int_0^{E_f} dE'\Sigma_s\left(E' \to E\right)\phi\left(E'\right) + \qquad (20a)$$
$$+ \int_{E_f}^{E_f/\alpha} dE'\Sigma_s\left(E' \to E\right)\phi\left(E'\right) + S(E)$$

with $E_0 \equiv E_f/\alpha$, and in multigroup form

$$\Sigma_g \phi_g = \sum_{g'=1}^{G} \Sigma_{sgg'}\phi_{g'} + Q_g, \qquad (20b)$$

then the source,

$$Q_g \equiv$$
$$\equiv \int_{E_g}^{E_{g-1}} dE \int_{E_f}^{E_f/\alpha} dE'\Sigma_s\left(E' \to E\right)\phi\left(E'\right) + S_g$$

is composed of two terms. The first comes from the previous interval and the second is the imposed external source. If we assume that an asymptotic flux (C_0/E) prevails above E_f, then the first source term is just the transfer cross section from the interval $\left[E_f, E_f/\alpha\right]$ into the gth group,

$$Q_{gs} \equiv \frac{C_0 \Sigma_{sg'}}{1-\alpha} \int_{E_f}^{E_f/\alpha} \frac{dE'}{E'^2} \int_{E_g}^{E_{g-1}} dE\rho\left(E', E\right). \qquad (21)$$

We evaluate the integral expression in Eq.(21) from Eqs.(14) to (18) with the lower and upper limits $E_{g'}$ and $E_{g'-1}$ replaced by E_f and E_f/α respectively. Now, we can accommodate either an external or slowing down source or both.

3.1.4. Convergence in G

Figure 3 shows the flux variation in energy for an increasing number of groups from $G = 10$ to 160 for the elastic scattering energy region of ^{12}C with a constant cross section for a source at $100ev$. Using the alternative CAC multigroup solution, we correctly predict the expected $1/E$ flux behavior and the Placzek transient. Also, as expected, the

approximation becomes increasing more faithful with increasing number of groups. Convergence seems to degrade however at lower energy. This demonstration confirms the new analytical generation procedure at least for constant cross section elastic scattering and that the multigroup approximation will eventually converge. The same analytic group parameter generation procedure is applicable to a single level Breit-Wigner resonance formulation.

4. **Final remarks**

A new solution to the slowing down equations using mathematical embedding, provide an independent solution to the **COMBINE7** spectral code. We compared the solution to the **COMBINE**7 solution indicating excellent results for a resonance calculation. A second investigation, which used analytically generated group parameters, investigated convergence in *G*. While convergence was demonstrated, additional study should be performed to derive a figure of merit for convergence.

References

Grimesey, R.A., Nigg, D.W., and Curtis R.L., COMBINE Version 7 is based on-- 1990. **COMBINE-5/PC** Manual, EG&G Idaho, Inc.

Fairen, V. et al., 1988. Power series approximation to solutions of nonlinear systems of differential equations, *Am J. Phys.*, **56**, 1.
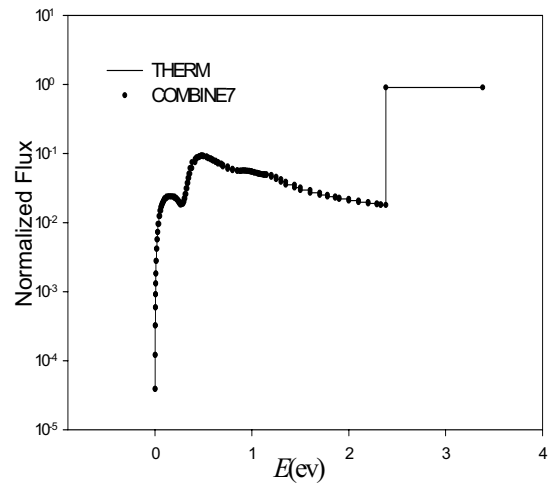
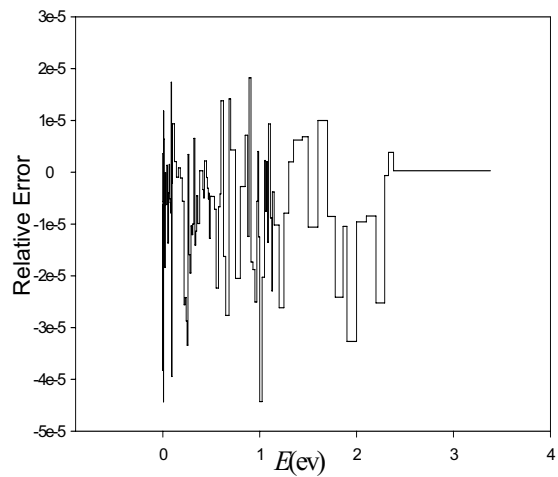Figure 1a COMBINE7/THERM comparison for Pu-239 resonance at 0.2956ev

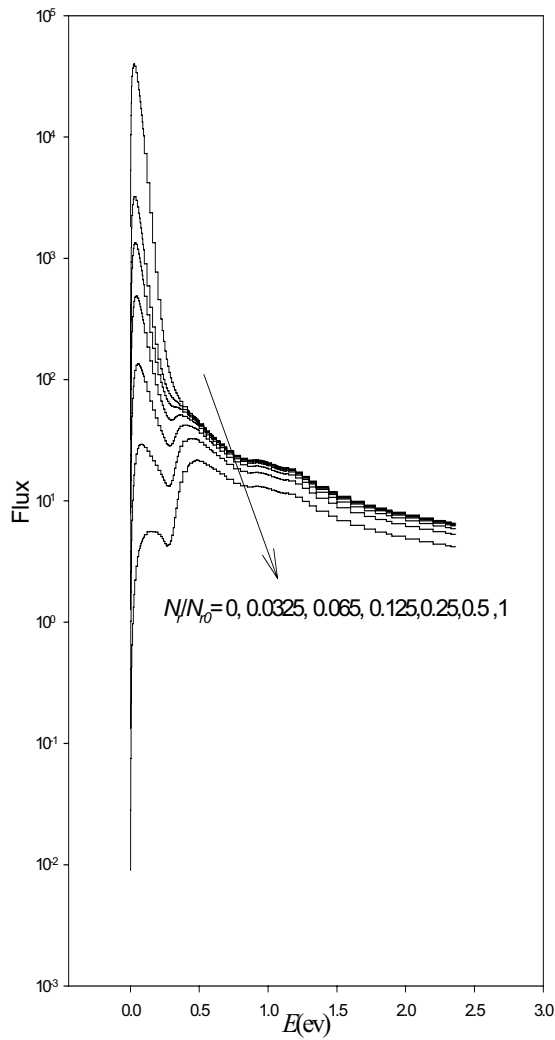Figure 1b Corresponding relative error between COMBINE7 and THERM

Figure 2 Approach to Pu-239 resonance with increasing fuel concentration

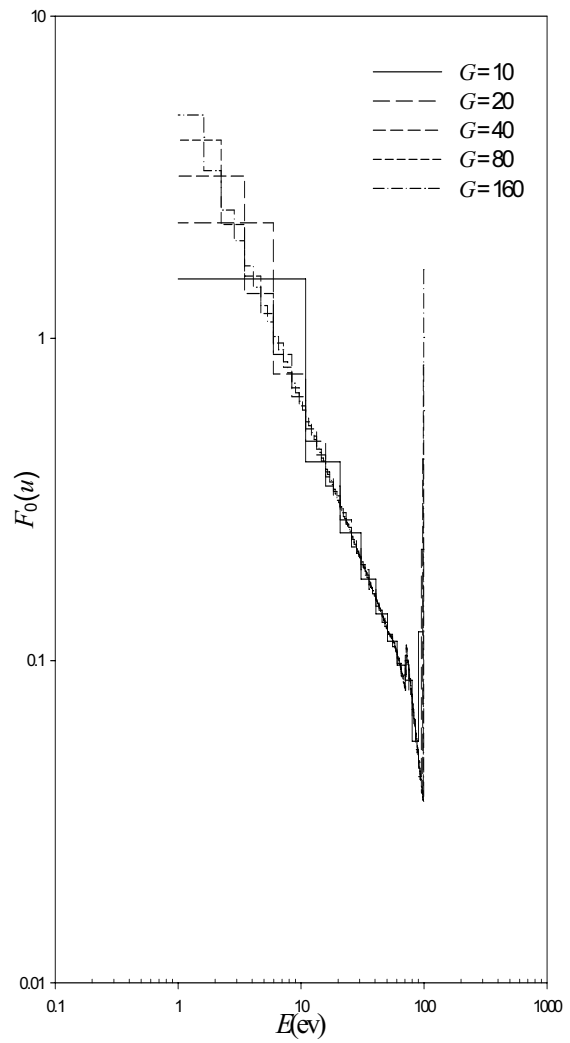N_f/N_{r0} = 0, 0.0325, 0.065, 0.125, 0.25, 0.5, 1

Figure 3 Elastic scattering for C-12 for an increasing number of groups

G = 10
G = 20
G = 40
G = 80
G = 160